Metallike Behavior of Lithium Intercalated in Molybdenum Cluster Chalcogenides

C. Prigge and W. Müller-Warmuth*

Institut für Physikalische Chemie der Westfälischen Wilhelms-Universität Münster, Germany

E. Gocke and R. Schöllhorn

Institut für Anorganische und Analytische Chemie der Technischen Universität Berlin, Germany

Received May 12, 1993. Revised Manuscript Received July 21, 1993®

^{7}Li solid-state NMR studies have been carried out on the molybdenum cluster chalcogenides ("Chevrel phases") $Li_3Mo_6X_8$, $Li_{3.8}Mo_6X_8$, and $Li_4Mo_6X_8$ at 16 and 117 MHz and various temperatures. The low-temperature spectra of $Li_3Mo_6X_8$, $Li_{3.8}Mo_6X_8$, and $Li_4Mo_6X_8$ can be interpreted in terms of chemical shift (CS), nuclear quadrupole (Q), and dipole–dipole (D) interaction, where the principal axes of the CS and Q tensors do not coincide. The spin–lattice relaxation of these compounds is governed by contributions from the lithium diffusion and from the interaction with conduction electrons. The latter part is connected with the isotropic (Knight) shift by a Korringa relation. The formation of lithium triclusters with partial charge transfer to the host lattice, short Li–Li distances and remaining electron density in the 2s orbitals is concluded from the various data. In $Li_4Mo_6X_8$, by contrast, the intercalated lithium is completely ionized. Models for structure and motion have been developed in connection with recent neutron diffraction studies.

Introduction

Binary and ternary molybdenum cluster chalcogenides (Chevrel phases) with the composition Mo_6X_8 and $A_xMo_6X_8$ (A = main group or transition metal; X = S, Se) have attracted considerable interest due to their unusual structure and dynamics and their remarkable physical properties such as superconductivity with high critical temperature and high critical magnetic fields.[1,2] For the intercalation compounds, both the chemical and the physical properties depend largely on the nature of the metal A and the degree of intercalation x. Compounds with intercalated lithium were investigated especially well. Four distinct phases with $x = 1, 3, 3.8$, and 4 were identified from the isotropic chemical shift of the ^{7}Li NMR.[3,4] Detailed studies of $Li_1Mo_6X_8$ revealed that more or less isolated Li^+ ions reside in one of six tetrahedral sites arranged on a plain inner ring within the cavities around the unit cell origin, and jumps between such positions take place.[5,6]

The $Li_3Mo_6X_8$ phase, in contrast, behaves completely different. The unusually large chemical shift suggested a partial charge transfer from the intercalated lithium to the host lattice and a clustering of three lithium atoms in the cavities.[3] The present paper aims at a detailed understanding of the structure and dynamics of this peculiar phase in which the intercalated species seem to possess many characteristics of a metal. It was furthermore our goal to study the transition to the lithium-rich phases $Li_{3.8}Mo_6X_8$ and $Li_4Mo_6X_8$ where the abrupt change to the latter compound is connected with a metal/semiconductor transition and the intercalated atoms become again completely ionized. Parallel to this solid-state NMR investigation, Ritter carried out high-resolution neutron diffraction measurements which were separately published.[6]

The compounds $Li_3Mo_6S_8$, $Li_3Mo_6Se_8$, $Li_{3.8}Mo_6S_8$, $Li_4Mo_6S_8$, and $Li_4Mo_6Se_8$ were prepared by topotactic redox reactions as described previously.[3] For control purposes the lithium content was checked by acid/base titration after the decomposition of the phases in distilled water, and furthermore samples prepared electrochemically were found to be identical with those synthesized by reaction of Mo_6X_8 with butyllithium. X-ray powder measurements were made by the Simon–Guinier technique from samples sealed in glass capillaries.

Experimental NMR Results

The ^{7}Li NMR measurements were carried out at 116.64 and 16 MHz using a Bruker CXP 300 FT-spectrometer with an additional electromagnet for the low field measurements. Solid state echo sequences $90°_x-\tau_{echo}-90°_y-\tau_{echo}$ were applied to obtain the spectra, which become rather broad at low temperatures. 90° pulse lengths were in between 5 and 8 μs. Spin–lattice relaxation times were measured employing $90°_x-\tau-90°_x-\tau_{echo}-90°_y-\tau_{Echo}-$ pulse sequences. The relaxation functions appeared to be exponential and could be fitted by one single relaxation time T_1. Exceptions are the compounds $Li_4Mo_6X_8$, where important nonexponentialities and rather long relaxation times were observed. Liquid nitrogen and in some cases liquid-helium cryostats were used to control the temperature.

Figure 1 shows a typical temperature dependence for two of the observed spectra. For all materials, above about 120 K line narrowing occurs and the anisotropic interactions become averaged. The (downfield) isotropic chemical shifts increase

* Abstract published in *Advance ACS Abstracts*, September 1, 1993.

(1) Yvon, K. *Curr. Top. Mater. Sci.* **1979**, *3*, 53.
(2) Fischer, Ø.; Maple, M. B. *Top. Curr. Phys.* **1982**, *32*.
(3) Gocke, E.; Schöllhorn, R.; Aselmann, G.; Müller-Warmuth, W. *Inorg. Chem.* **1987**, *26*, 1805.
(4) Aselmann, G.; Müller-Warmuth, W.; Gocke, E.; Schöllhorn, R. *Z. Phys Chem.* **1987**, *151*, 103.
(5) Prigge, C.; Müller-Warmuth, W.; Gocke, E.; Schöllhorn, R. *Solid State Ionics*, in press.
(6) Ritter, C.; Gocke, E.; Fischer, C.; Schöllhorn, R. *Mater. Res. Bull.* **1992**, *27*, 1217.

0897-4756/93/2805-1493$04.00/0

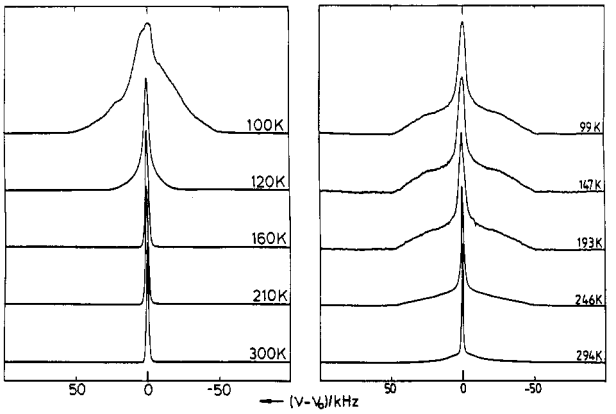

Figure 1. Temperature dependence of the experimental ^{7}Li NMR spectra of $Li_3Mo_6S_8$ (left) and $Li_4Mo_6S_8$ (right). The measurements were carried out at 116.64 MHz; the zero of the calibrated base-line does not take into account the isotropic chemical shifts, which are given in Table I.

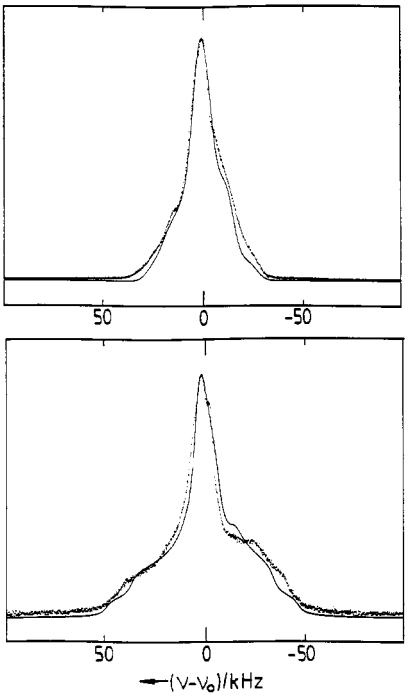

Figure 2. Experimental ^{7}Li NMR spectra of the $Li_3Mo_6X_8$ compounds (116.64 MHz, 100 K) and their simulations (top, X = S; bottom, X = Se).

about linearly with decreasing temperature from 78 ppm at 300 K to 94 ppm at 100 K ($Li_3Mo_6S_8$), respectively from 87 ppm to 111 ppm ($Li_3Mo_6Se_8$), and from 22 to 40 ppm ($Li_{3.8}Mo_6S_8$). All these values are referred to an aqueous solution of LiCl; they are less accurate at low temperatures where the spectra are very broad. In particular for $Li_{3.8}Mo_6S_8$ the chemical shift value varies somewhat from sample to sample. $Li_4Mo_6S_8$ and $Li_4Mo_6Se_8$, by contrast, display constant isotropic shifts of 0 and 3 ppm, respectively.

Information on the static structure was obtained from the dipolar, quadrupolar and anisotropic chemical shift interactions at low temperatures. Figures 2–4 show the rather complex experimental spectra at 117 MHz and their simulations (cf. next paragraph). The ^{7}Li NMR spectra at 16 MHz were also recorded; they are less good, but they are important to confirm the interpretation.

The dynamic behavior of the guest phases was examined by the line narrowing process of the spectra, but first of all by measurements of the spin–lattice relaxation rates. $1/T_1$ plotted versus reciprocal temperature shows the same characteristic behavior for the phases $Li_3Mo_6X_8$ and $Li_{3.8}Mo_6X_8$ (Figures 5 and

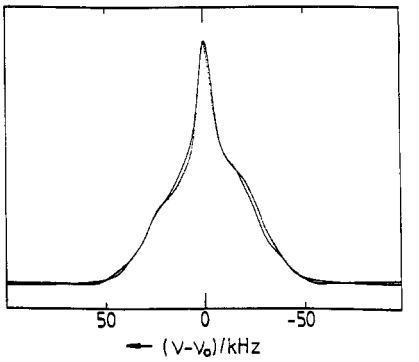

Figure 3. Same as Figure 2, but for $Li_{3.8}Mo_6S_8$.

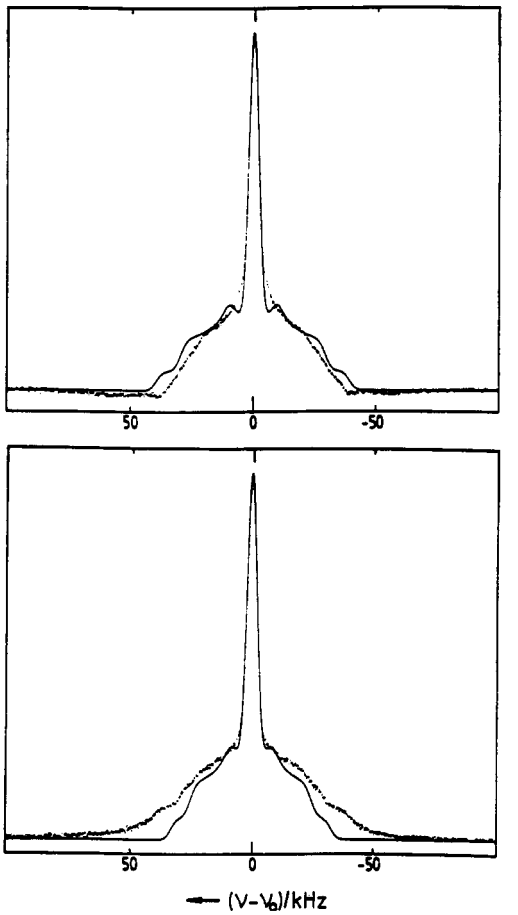

Figure 4. Same as Figure 2, but for the $Li_4Mo_6X_8$ compounds (top, X = S; bottom, X = Se).

6): a diffusion maximum superimposed on a relaxation term which increases with temperature. For $Li_4Mo_6X_8$ (not shown), below about 200 K T_1^{-1} is very small and constant (X = S, 0.002 s^{-1}; X = Se, 0.01 s^{-1}), it starts then to increase and reaches values between 0.1 and 0.5 s^{-1} at 300 K.

Interpretation

Spectral Line Shapes. The broad and asymmetric spectra of the phases $Li_3Mo_6X_8$ and $Li_{3.8}Mo_6X_8$ (Figures 2 and 3) are the result of a simultaneous anisotropic chemical (or Knight) shift and nuclear quadrupole interaction combined with dipolar broadening. A detailed inspection shows that the principal axes of the chemical shift and electric field gradient (EFG or quadrupole interaction) tensors do not coincide. The line-shape simulations were therefore accomplished using the following expression for the transition frequency from a state

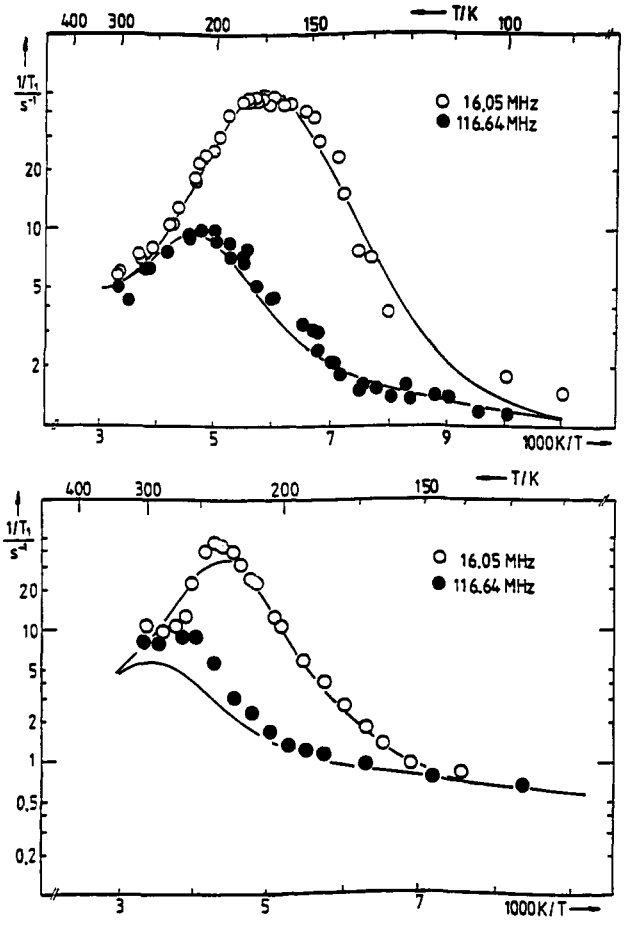

Figure 5. Spin–lattice relaxation rates versus reciprocal temperature for $Li_3Mo_6S_8$ (top) and $Li_3Mo_6Se_8$ (bottom). The solid curve corresponds to the theoretical description described in the text.

m to a state $m - 1$:

$$\omega = \omega_0(1 + \sigma_{iso}) + {}^1/_6\omega_0\Delta\sigma\{3\sin^2\beta\sin^2\vartheta\cos 2\varphi - 3\sin 2\beta\sin 2\vartheta\cos\varphi + (3\cos^2\beta - 1)(3\cos^2\vartheta - 1) - \eta_{cs}[{}^1/_2(1 + \cos\beta)^2\sin^2\vartheta\cos 2(\varphi + \gamma) + {}^1/_2(1 - \cos\beta)^2\sin^2\vartheta\cos 2(\varphi - \gamma) + (1 + \cos\beta)\sin\beta\sin 2\vartheta \times \cos(\varphi + 2\gamma) - (1 - \cos\beta)\sin\beta\sin 2\vartheta\cos(\varphi - 2\gamma) + \sin^2\beta\cos 2\gamma(3\cos^2\vartheta - 1)]\} + \frac{3e^2qQ}{4I(2I-1)\hbar}\left(\frac{1}{2} - m\right)[3\cos^2\vartheta - 1 - \eta_Q\sin^2\vartheta\cos 2\varphi] \quad (1)$$

The meaning of the symbols is as usual. The absolute value of σ_{iso}, the isotropic chemical shift, is negative, but only relative values referred to LiCl will be given. The chemical shift (CS) anisotropy $\Delta\sigma = \sigma_{zz} - (\sigma_{xx} + \sigma_{yy})/2$ and quadrupole (Q) coupling constant e^2qQ, as well as the asymmetry parameters η_{CS} and η_Q are in each case defined in their own principle axis system (PAS). The PAS of the electric field gradient (EFG, or nuclear quadrupole interaction) is oriented with respect to the laboratory frame (determined by the direction of the applied magnetic field B_0) by the polar angle ϑ and the azimuthal angle φ. The powder spectrum is obtained from a weighted integration over ϑ and φ as usual. Calculations were carried out applying the algorithm published by Alderman et al.[7]

(7) Alderman, D. W.; Solum, M. S., Grant, D. M. *J. Chem. Phys.* **1986**, *84*, 3717.

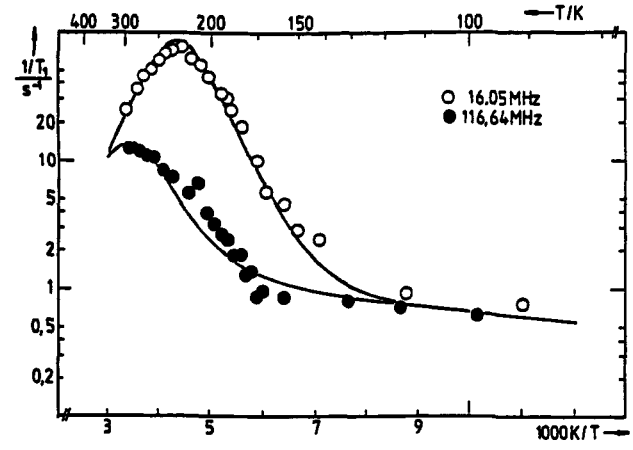

Figure 6. Same as Figure 5, but for $Li_{3.8}Mo_6S_8$.

Table I. NMR Parameters Describing the Various Interactions and the Relative Positions of the PASs of the Chemical Shift and Quadrupole Coupling As Obtained from the Spectra Simulations[a]

parameter	$Li_3Mo_6S_8$	$Li_3Mo_6Se_8$	$Li_{3.8}Mo_6S_8$	$Li_4Mo_6S_8$	$Li_4Mo_6Se_8$
σ_{iso}/ppm	94 ± 5	111 ± 5	39 ± 5	0 ± 5	3 ± 5
$\Delta\sigma$/ppm	−113 ± 7	−90 ± 10	−45 ± 5		
η_{cs}	0	0	0		
e^2qQ/h/kHz	75 ± 5	95 ± 5	81 ± 3	65 ± 3	78 ± 3
η_Q	0.25 ± 0.15	0.50 ± 0.15	0.4 ± 0.1	0.5 ± 0.1	0.5 ± 0.1
β/°	55 ± 10	55 ± 10	55 ± 5		
γ/°	90 ± 10	90 ± 10	90 ± 5		
$\Delta\nu_D$/kHz	8.2 ± 0.3	4.2 ± 0.3	5.9 ± 0.2	4.7 ± 0.2	4.7 ± 0.2

[a] The uncertainties are related to the influence of the respective quantity on the fit.

The Eulerian angles β and γ can be determined from the experimental spectra by simulation using eq 1. β is the angle between the z axes of the EGF and CS tensors. The projection of the z axis of the EFG tensor on to the azimuthal plane of the PAS of the CS makes the angle γ with the x axis of the latter. A knowledge of these angles is quite helpful for explaining the structural arrangement. In this place we omit to present the derivation of eq 1, since in the meantime analogous treatments were published by other authors.[8,9]

The results of the best fitting computer simulation of the experimental spectra is indicated by the solid lines of Figures 2 and 3. The corresponding parameters are listed in Table I. Another pecularity are the dipolar broadenings which can be described in high field better by Lorentzians rather than Gaussians and which grow upon increasing the resonance frequency. The values given in Table I refer to the full dipolar width at half-height (fwhh) of a Gaussian determined at the low frequency of 16 MHz.

The spectra of $Li_4Mo_6S_8$ and $Li_4Mo_6Se_8$ (Figure 4) look less complex. Chemical shift interactions are negligible and dipolar broadenings can be taken into account by folding the powder patterns with frequency independent Gaussians of appropriate width. The spectra are governed by nuclear quadrupole interactions of first order. The simulations with the corresponding parameters are given in Figure 4 and Table I.

Although the spectra are governed by various parameters the simulations cannot be perfect. This depends in part on experimental influences, and in part on certain details of the curves which are not sensitive to the parameter

(8) Cheng, J. T.; Edwards, J. C.; Ellis, P. D. *J. Phys. Chem.* **1990**, *94*, 553.

(9) France, P. W., *J. Magn. Reson.* **1991**, *92*, 30.

Table II. Parameters Connected with the Lithium Diffusion and the Interaction with 2s Conduction Electrons As Obtained from the Spin-Lattice Relaxation Data[a]

	$Li_3Mo_6S_8$	$Li_3Mo_6Se_8$	$Li_{3.8}Mo_6S_8$
E_A/(kJ/mol)	13 ± 2	19 ± 3	17 ± 2
$\tau_{co}/10^{-13}$ s	4.6 ± 1.0	2.9 ± 1.5	5.0 ± 1.0
$C_1/10^9$ s^2	3.6 ● 0.5	2.3 ± 0.6	5.9 ± 0.8
$C_2/10^{-2}$ s K	1.2 ± 0.3	0.56 ± 0.20	0.65 ± 0.15
$K^2T_1/1/T/10^{-6}$ s K	0.88 ± 0.10	2.65 ± 0.50	0.32 ± 0.05

[a] The uncertainties are connected with the data fits by eq 2.

values. The quantities given in Table I are not equally sensitive to all details of the curves; some appear to be rather certain, others are only estimates (cf. the uncertainties indicated in Table I). The conclusions are decisive, but a better fit does not depend on the number of parameters.

Relaxation. The experimental ^{7}Li NMR spin-lattice relaxation rates, Figures 5 and 6, are characteristic of both diffusional motion with frequency-dependent maxima and interaction of the lithium nuclei with conduction electrons. The latter mechanism leads to a relaxation rate which increases with temperature. A reasonable approach would just be to add the contributions of each mechanism:[10]

$$\frac{1}{T_1} = C_1\left[\frac{\tau_c}{1+\omega_0^2\tau_c^2} + \frac{4\tau_c}{1+4\omega_0^2\tau_c^2}\right] + C_2T \qquad (2)$$

as shown by the solid curves through the points. Both relaxation strengths (C_1, C_2), the activation energy E_A and the preexponential factor τ_{co} for the motion as obtained from the best fits are given in Table II. The description of the data by eq 2 looks rather well for $Li_3Mo_6S_8$ and $Li_{3.8}Mo_6S_8$. It is less good for $Li_3Mo_6Se_8$, where the BPP function is not appropriate as already observed for several other guest phases in intercalation compounds (cf. e.g., ref 11). We did not attempt to improve the fit by choosing another spectral density function, because the separation of several contributions does not secure the necessary accuracy for such a procedure. Both an improved spectral density and the introduction of further correction terms would of course reduce the uncertainties of the parameters given in Table II. In any way, the parameters of Table II give the correct picture and describe the behavior of the intercalated lithium species. It is also clear from the high-temperature data that the motion does not display elements of low dimensionality.

The second contribution $1/T'_1 = C_2T$ appears to be closely related to the isotropic chemical shift. If the product $\sigma_{iso}^2T'_1$ is plotted versus reciprocal temperatures, as shown in Figure 7 for one of the compounds, a straight line can be drawn through the points. This suggests that the "Korringa relationship" is fulfilled, i.e., the product $K^2T'_1T$ is constant (K = Knight shift). We may therefore identify the essential part of σ_{iso} as a Knight shift due to the interaction with metallic electrons. The values of the Korringa product calculated from the slope of the lines of Figure 7 and corresponding representations for the other compounds are also given in Table II.

They are not far from those of the theoretical relation for a Fermi gas,[10,12] which is known to be very approximative:

$$K^2T_1T = \frac{\hbar}{4\pi k}\left(\frac{\gamma_s}{\gamma_I}\right)^2 \qquad (3)$$

The magnetogyric ratios γ refer either to electronic (S) or nuclear spins (I). For lithium nuclei and s electrons, eq 3 gives 1.8×10^{-6} s K.

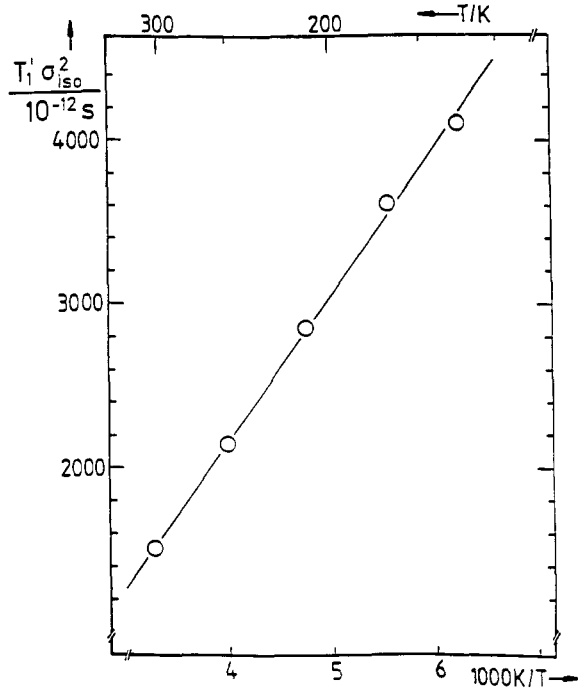

Figure 7. Korringa product for $Li_3Mo_6S_8$ plotted versus reciprocal temperature.

It has to be emphasized that neither K nor T_1T is independent of temperature as expected in a simple metal. But the individual dependences cancel if the Korringa product is formed. We attribute this behavior to the motional effects. The individual Li_3 clusters (cf. discussion of the next section) are permanently broken by the diffusion of the lithium species.

Discussion

$Li_3Mo_6X_8$. Both the existence of the relative large Knight shift and the relaxation behavior show the exceptional role of the $Li_3Mo_6X_8$ phase within the $Li_xMo_6X_8$ system. The tentative suggestion of a formation of Li_3^{z+} clusters ($0 < z < 3$) with partial charge transfer to the host lattice[3] can be confirmed. Some remaining electron density in the 2s orbitals of the intercalated lithium atoms is responsible for the effects. Further evidence of this are the specific properties of the chemical (=Knight) shift anisotropy and the dipolar broadening.

For all the $Li_3Mo_6X_8$ and $Li_{3.8}Mo_6X_8$ compounds the Knight shift tensor is axially symmetric with $\Delta\sigma$ being relative large and negative (cf. Table I). Knowing the host lattice structure and the framework of potential lithium sites on the two rings around the unit cell origin (Figure 8), the z axis of this tensor may be identified therefore with the symmetry axis perpendicular to the plane spanned by these two rings with three potential tetrahedral sites each. That part of the 2s electron density which is not transferred to the host lattice appears to be distributed symmetrically about the axis. The sign of $\Delta\sigma$ indicates more screening (and bonding) electron density in the plane rather than below and above the lithium nuclei. A peculiarity of $Li_3Mo_6X_8$ as compared with the other members of the $Li_xMo_6X_8$ system is the enlargement of the inner ring resulting in a remarkable Li1–Li1 next-neighbor separation of 230 pm and a considerable short-

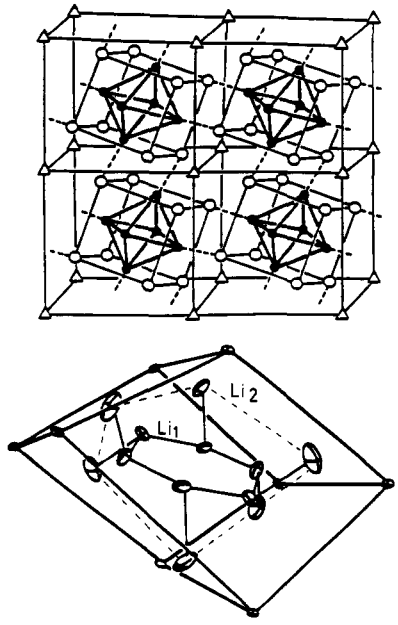

Figure 8. Top: structure scheme of binary molybdenum cluster chalcogenides Mo_6X_8 (● = Mo, ○ = X, △ vacant channel positions). Bottom: two times six potential lattice sites Li1 and Li2 arranged on two concentric rings around the unit cell origin, *cf.* refs 1 and 2.

ening of the Li1–Li2 distance.[6] A sufficient number of lithium sites arranged symmetrically is therefore available, so that triclusters with short Li–Li distances can be formed.

While the principal axis of Knight shift tensor is given by the 2s electron distribution within the planes of the lithium sites, the directional dependence of the EFG tensor is attributed to the symmetry of the host lattice. The principal axis system of the EFG seems to agree with the rhombohedral reference system of the structure. Then the angles β and γ describing the relative positions of the noncoincident principal axes systems of the EFG and Knight shift tensors should become 54.54° and 90°, respectively, as observed. The quadrupole coupling constant has the same order of magnitude for all the compounds including $Li_1Mo_6X_8$.[5] The EFG tensor is not axially symmetric and determined by the host lattice contribution. The lattice distortions are similar for all the ternary compounds of the $Li_xMo_6X_8$ system.

Within the $Li_xMo_6X_8$ system, the magnetic field dependence of the dipolar linewidth is restricted to $Li_3Mo_6X_8$ and $Li_{3.8}Mo_6X_8$ where the interaction with metallike electrons plays a role. At 16 MHz in a relative low field the remaining width is practically only due to dipole–dipole interactions between the nuclear moments of the lithium nuclei. This coupling is very small for $Li_1Mo_6X_8$ where at most one lithium ion resides in a cavity,[5] but sufficiently important for the compounds of the present study. Rigid lattice values were observed at temperatures of 100 K and below (cf. Figure 1). Application of the van Vleck formula[10] leads to an estimate of 210 pm (370 pm) for the Li–Li separation in $Li_3Mo_6S_8$($Li_3Mo_6Se_8$) if two next neighbors at the same distance and 18 and 36 lithium nuclei at the distance a of the lattice constant, and $\sqrt{2}a$, respectively, are assumed. These findings agree well with the high-resolution neutron diffraction results of Ritter for $Li_3Mo_6S_8$[6] specifying shortest Li1–Li1 distances of 230 pm, Li1–Li2 distances of about 400 pm, but rather short Li1–Li2 separations. As a conclusion, the Li_3^{2+} cluster may be expected to occupy essentially sites on the enlarged inner ring.

Figure 5 and Table II, as well as the line narrowing of Figure 1, show that motions which modulate the various interactions are easily activated. The motional contribution of the spin–lattice relaxation is essentially created by the time dependence of the nuclear quadrupole coupling to the lattice as may be concluded from the numerical values of C_1. The mechanism must be a translational diffusion from cavity to cavity. The neutron diffraction data explain why the Li mobility is that high, also as compared with $Li_1Mo_6X_8$ and $Li_4Mo_6X_8$.[6] The enlargement of the inner ring provides a framework of symmetrically arranged potential sites with short and comparable distances. A symmetric Li_3 cluster can easily be transformed from inner to outer sites. Nearly equidistant positions including intracluster and intercluster steps are available as a possible lithium diffusion pathway.

$Li_{3.8}Mo_6S_8$. In contrast to stoichiometries of the $Li_xMo_6X_8$ system with $3 < x < 3.8$ where two NMR signals appear, by the presence of only one narrow NMR line at room temperature, the $Li_{3.8}Mo_6X_8$ compounds are clearly identified as single-phase systems. Both the isotropic and anisotropic Knight shifts are present, but less important than in $Li_3Mo_6X_8$. All the other NMR data are comparable. Apart from the fact that these materials are not quite so stable they behave very much like the $Li_3Mo_6X_8$ compounds. In particular, they share the exceptional role to show interactions of the lithium nuclei with conduction electrons, even though the electron density may be less. The lithium mobility is rather high as well depending on the availability of similar pathways for the diffusion. From the linewidths, somewhat larger mean Li–Li distances of the order of 330 pm were estimated. This agrees with the neutron diffraction result that the relative occupancy of sites on the outer ring is obviously larger.[6]

$Li_4Mo_6X_8$. The behavior of the fully intercalated phase is in every respect different from that of the compounds discussed so far. There is no longer any Knight shift; the isotropic chemical shift corresponds to that of Li^+ ions and the chemical shift anisotropy is negligible. The low-temperature ^7Li NMR spectra are governed by quadrupole and dipole–dipole interactions. Deviations of the experimental spectra from the simulations (Figure 4) concern a certain smearing of the satellite transitions indicating a distribution of surroundings of the intercalated lithium ions. In agreement with the neutron diffraction data[6] a structure model may apply where, on the average, the inner sites are still occupied by one atom per ring, and the outer sites by the remaining three guest atoms. The dramatic transition from $Li_3Mo_6X_8$ (and even $Li_{3.8}Mo_6X_8$) to $Li_4Mo_6X_8$ as observed by NMR and manifested itself by the macroscopic properties can also be realized from the structure. The inner ring is no longer enlarged, and there is a large separation between inner Li1 and outer Li2 sites comparable with $Li_1Mo_6X_8$.[6] From the point of view of NMR, $Li_4Mo_6S_8$ and $Li_4Mo_6Se_8$ are not much different.

The lithium mobility is much less in $Li_4Mo_6X_8$ as compared with $Li_3Mo_6X_8$ and $Li_{3.8}Mo_6X_8$. This may be explained in terms of the available sites for the diffusion pathway which are no longer separated by comparable

(10) Abragam, A., *The Principles of Nuclear Magnetism*; Clarendon Press: Oxford, 1961, and other textbooks on NMR.
(11) Ritter, C.; Müller-Warmuth, W.; Schöllhorn, R. *J. Chem. Phys.* **1985**, *83*, 6130.
(12) Korringa, J. *Physica* **1950**, *16*, 601.

distances. The appearance of motions is indicated by the line narrowing process (Figure 1), but the diffusion is slow and more difficult to activate, since the relaxation maximum is not accessible.

Conclusions

The ^{7}Li solid-state investigations of the $Li_xMo_6X_8$ system, in connection with recent high-resolution neutron diffraction studies, lead to a reasonable description of the four distinct phases whose properties differ so much. In $Li_1MoX_6X_8$ and $Li_4Mo_6X_8$ the intercalated lithium is ionized and the charge transfer to the host lattice is complete. Apart from the local motion in $Li_1Mo_6X_8$, the lithium mobility is small. In $Li_3Mo_6X_8$ and $Li_{3.8}Mo_6X_8$, by contrast, lithium clustering takes place in the guest phase, and the metallike behavior of the intercalated lithium is established by several experiments. In these phases the lithium mobility is high. These findings are accompanied by adequate changes of the framework of potential sites on the concentric inner and outer rings around the unit cell origin.